Research Article

Butyl rubber-based composite: Thermal degradation and prediction of service life time

Phuong Nguyen-Tri [1] *, Ennouri Triki[2], Tuan Anh Nguyen[3]

[1] Department of Chemistry, University of Montreal, Montreal, Quebec, Canada; phuong.nguyen.tri@umontreal.ca
[2] Department of Mechanical Engineering, McGill University, Montreal, Quebec, Canada; ennouri.triki@mail.mcgill.ca
[3] Institute for Tropical Technology, Vietnam Academy of Science and Technology (VAST), Hanoi 122100, Vietnam; ntanh2007@gmail.com

* Correspondence: phuong.nguyen.tri@umontreal.ca ; Tel.: + 514-340 5121 (7326)

Abstract: Butyl rubber-based composite (BRC) is one of the most popular materials for the fabrication of protective glove against chemical and mechanical risks. However, in many working places such as metal manufacturing or automotive mechanical services, its mechanical hazards usually appear together with metalworking fluids (MWFs). The presence of these contaminants, particularly at high temperature, could modify its properties due to the scission, the plasticization, the crosslinking of polymer network and thus led to severe modification of mechanical and physicochemical properties of material. This work aims to determine the effect of temperature and a metalworking fluid on mechanical behavior of butyl rubber composite dealing with crosslinking density, cohesion forces and elastic constant of BRC on the based on Mooney-Rivlin's theory. The effect of temperature with and without MWFs on thermo dynamical properties and morphology of butyl membranes is also investigated. The prediction of service lifetime is then evaluated from extrapolation of Arrhenius plot at different temperatures.

Keywords: Polymer aging, swelling behavior, protective glove materials, elastomers, composites, rubber

1. Introduction

Rubber is one of the most important materials for various industries, especially in petroleum, construction [1] and protection material sectors [2, 3]. Protective gloves are often covered by an elastomeric coating to protect against chemical and mechanical damages due to its good resistance to abrasion, oils, chemicals and its excellent damping properties [4-12]. However, the swelling phenomena involving the degradation of the mechanical properties of these materials have often been observed [13]. Butyl rubber-based composite (BRC) is one of the most effective materials against chemical risks [4, 13]. However, this material is sensitive to nonpolar solvents or metalworking fluid. These non-polar compounds can easily penetrate in the polymer and lead a dramatically change of material properties. These problems represent a large risk for users and thus require a better understanding of the problem [13, 14]. Like other polymers, butyl rubber-based composites can be affected by oxidation and this effect becomes more intensive at high temperature.

The swelling characteristics of rubbers are related to the deterioration of mechanical properties and may affect to their failure mechanics. Nowadays, there are no models to predict the failure

Preprints (www.preprints.org) | NOT PEER-REVIEWED | Posted: 15 April 2019 doi:10.20944/preprints201904.0163.v1

mechanisms in the presence of industrial contaminants. Several investigations have been reported on the effect of industrial contaminants on morphology, mechanical properties and structure of gloves material. In previous works [15-24], we reported that polymers and composites [16-20, 22, 23, 25-41] can be degraded by several aging agents such as heat, water, humidity, oxygen, ozone and various other environments factors [16-24]. The scission, crosslinking and plasticization of polymer network may be occurred and led to severe deterioration of mechanical and physicochemical properties of material [42], which are quite important as regards their applications in various fields of mechanical engineering.

Many researchers have been attempted to understand the relationship between morphological and property changes with microstructure of rubber material[43], especially with failure mechanism of elastomer by using several traditional test methods including tensile test, strain-stress relation, and compression measurements [44-46]. Mooney-Rivlin's equation is usually used to evaluate the property-structure relationship of material by analysing of tensile stress-strain curves of materials. In this model, Rivlin [47, 48] proposed an extension of the Mooney's model by describing W as a polynomial series in (I_1 - 3) and (I_2 - 3):

$$W = \sum_{i.j=0}^{\infty} C_{ij} \left(I_1 - 3\right)^i \left(I_2 - 3\right)^j \quad \text{with } C_{00} = 0 \qquad \text{Eq.1}$$

During a simple tensile test, we are:

$$I_1 = \lambda^2 + \frac{2}{\lambda} \qquad I_2 = \frac{1}{\lambda^2} + 2\lambda \qquad I_3 = 1 \qquad \text{Eq.2}$$

The stress σ_n is given by the equation:

$$\sigma_n = 2\left(\lambda - \frac{1}{\lambda^2}\right)\left[\frac{\partial W}{\partial I_1} + \frac{1}{\lambda}\frac{\partial W}{\partial I_2}\right] \qquad \text{Eq.3}$$

According to the behavior law, we can still write:

$$\sigma_n = \lambda\frac{\partial W}{\partial \lambda_1} + \frac{1}{\lambda}\frac{\partial W}{\partial \lambda_2} \qquad \text{Eq.4}$$

From which

$$\sigma_n = 2\left(C_1 + \frac{C_2}{\lambda}\right)\left(\lambda - \frac{1}{\lambda^2}\right) \qquad \text{Eq.5}$$

where W is the density of deformation energy, λ is elongation of material and C_1 et C_2 are two elastic constants associated with network structure and the flexibility of network, respectively. According to Eq.5, plot of $\sigma_n / 2\left(\lambda - 1/\lambda^2\right)$ as a function of λ^{-1} should be a linear and the C_1 constant is directly calculated by extrapolating of the linear portion of the curve up to $\lambda^{-1} = 0$ and the C_2 constant is the curve slope. In the molecular aspect, this constant C_1 of Mooney-Rivlin's model characterizes by the density of crosslinking between elastomer chains [49, 50]. It can be used to evaluate the physical manifestation of the degree of crosslinking N [51, 52].

$$N = \frac{2C_1}{kT} \quad \text{Eq.6}$$

The constant C_2 is associated with the cohesion forces (intramolecular bonds and interchain) and reinforcement-matrix interactions[52]. This constant also reflects the flexibility of the structure of the material[53]. It depends on the degree of vulcanization which increases with the increasing of the crosslink density[53]. The values of two constants C_1 and C_2 that can be determined during the tensile tests allow for studying the influence of the crosslinking degree and network structure on the stiffness of material. Gordon [52] is determined the Young's modulus according to C_1 and C_2:

$$E = 6\left(C_1 + C_2\right) \quad \text{Eq.7}$$

It reported that the constant C_1 usually remains constant with variation of the swelling degree of polymer material, while the constant C_2 decreases with the increase of swelling degree[54-56]. It lacks a systematically research on the effect of temperature and metalworking on morphology, properties and structure of elastomer materials.

In this study, a butyl rubber membrane, representing a common material used in protective gloves, has been used to determinate the swelling characteristics to metalworking fluid at various temperatures ranging from 80 °C to 120 °C. The elastic behaviors dealing with elastic constants, crosslinking density and modulus were continuously followed during the contamination procedure to evaluate the dominant parameter on polymer deterioration. The modification of morphology, tensile properties and physicochemical properties were also investigated.

2. Materials and Methods

2.1. Materials

Butyl rubber based composite (BRC) membranes used in this work are made from butyl rubber with carbon black fillers. These commercial products (thickness of ~1.6mm) are kindly supplied by MCMaster-Carr Inc. (Canada). An industrial MWF used in this work, namely Milform 64 SST, is directly purchased from a company in metalworking sector in Quebec, Canada. The chemical composition can be found in our previous publication. The carbon black filler content in composite membranes is estimated to be 42- 44 wt.% (by TGA measurement).

2.2. Contamination procedure

The elastomer membranes having the mass (m_0) were immersed in to the liquid contaminants for different periods of time for measuring of swelling index changes according to the ASTM D471-12 standard. They are then delicately wiped by thick wiping papers to remove the excess oil on sample surface and reweighed (m_t). The process is repeated until saturated state. The swelling index (M) is calculated according to the relation following:

$$M(\%) = \frac{m_t - m_0}{m_0} x100 \quad \text{Eq.8}$$

where m_o and m_t are respectively the weight of the samples before and after immersion in contaminant.

2.3. Scanning electron microscopy (SEM)

Scanning electron microscopy model Hitachi S570 was used to investigate the morphology and the fractography changes of samples before and after contamination process. These observations serve to examine the failure modes of morphology changes of elastomer materials.

2.4. Tensile tests

Tensile properties of elastomer membranes are measured with the dog bone rectangular samples. Measurements were performed with an Alliance 2000 (MTS) universal testing machine equipped with 1000N load cell and operated at a cross-head speed of 500 mm/min according to the ASTM D412-06 standard test method. For each condition, five replicates are measured.

2.5 Thermal gravimetric analysis (TGA)

TGA is carried out with original and aged composite samples to evaluate the percentage of filler content and the effect of aging process on the sample weight loss as a function of time. The TGA is carried out in nitrogen atmosphere at a heating rate of 20 ºC/min using a Parkin Elmer TGA model 4000. Thermograms were recorded from 0 to 800 ºC.

3. Results and discussions

3.1. Effect of temperature on mechanical properties

The influence of temperature on the viscoelastic properties of BRC is investigated at three different temperatures ranging from 80 and 120°C. Figure 1a shows the relationship between the constant C_1 and exposure time. It demonstrates that the highest value of constant C_1 is observed at temperature around of 120°C. At the beginning of exposure ($t < 4$ h), C_1 undergoes a significant increase, and then rapidly decreases before achieving a constant value. At lower exposure temperature (80°C and 100°C), the variation of the constant C_1 is not significant representing by a slight decrease of C_1 at the first exposure hours then appears to be converged to the similar value to that observed at 120°C. These results allow confirming that the stiffness of butyl is optionally increased with temperature, as reported in the case of a neoprene membrane which is exposed to high temperature [57]. Figure 1b shows the variation of C_2 as a function of exposure time at different temperatures. The variation of the constant C_2 at 80°C appears to be similar to that at 100°C with parabolic shape curve. An increase in C_2 at first hours of exposition ($t < 4$h) is observed and then it becomes to slightly decrease with the time. It can be attributed to the increase of cohesive force at the first hours of exposition time and then decrease [54]. This physical phenomenon is completely different to that observed at higher exposure temperature (120°C). The constant C_2 decreases significantly from the first steps of exposure and go down to zero. These results are not surprise and are in good agreement with that published by Marck [54].

Preprints (www.preprints.org) | NOT PEER-REVIEWED | Posted: 15 April 2019 doi:10.20944/preprints201904.0163.v1

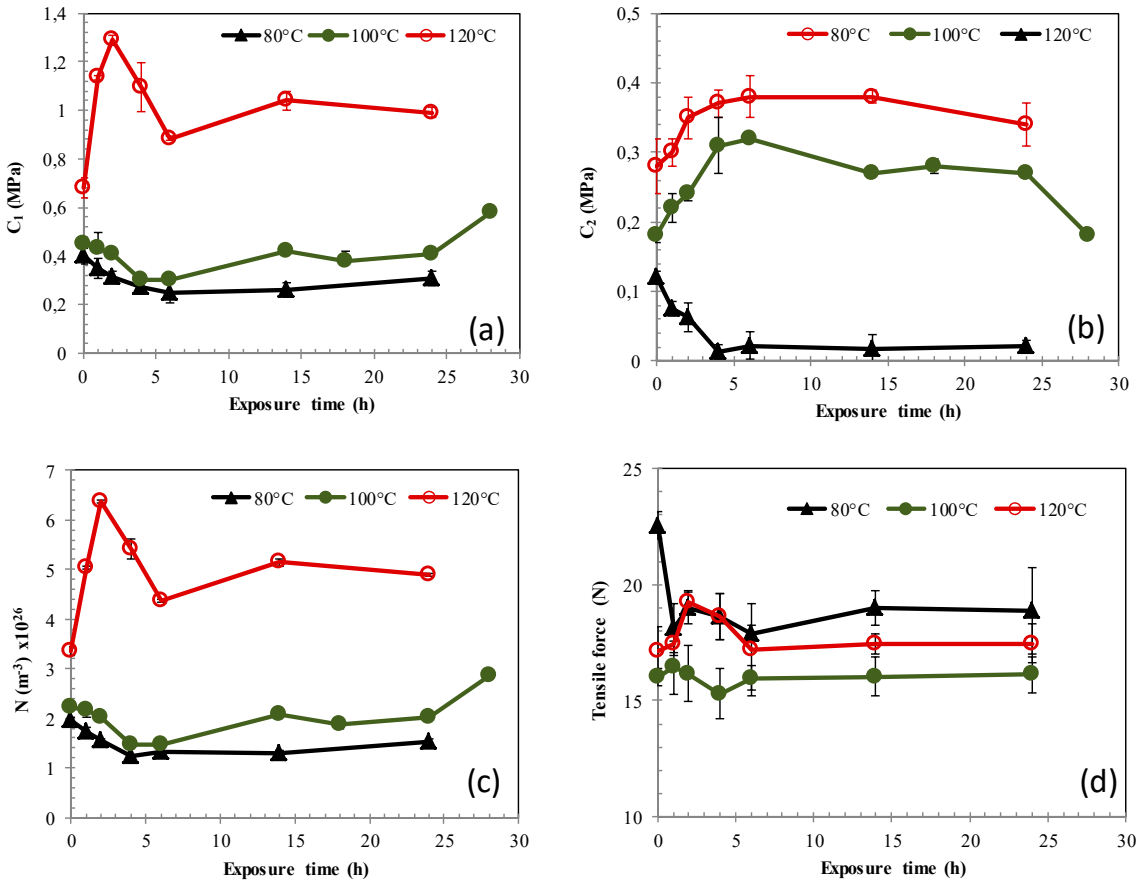

Figure 1 Effect of temperature on mechanical properties of BRC as function of MWF exposure time a) constant C_1; b) constant C_2; c) Crosslinking density (N); d) Tensile force.

The synergy the between the variation of C_1 and C_2 is also investigated and the results are shown in Table 1. This synergy is determined by calculating the theoretical Young's modulus by using Eq.7 and the experimental Young's modulus from the first linear region of the force-displacement curves (Fig. 1d). The obtained results show that the rigidity of the butyl remains almost unchanged at 80°C. However, a significant increase of Young's modulus with exposure time was recorded at 100°C and 120°C. This can be attributed generally to the increasing of crosslinking density (N) that may be occurred at high temperature due to the vulcanization or reticulation of polymer chains. After 24 hrs exposure in MWF, the Young's modulus seems to be increased for all studied temperatures (Fig 1c). Figure 1d demonstrates the tensile force of BRC as a function of exposure time, it can be seen that the rupture properties remain constant during all exposure times whatever the exposure temperature. The variation of tensile strength at break with exposure time is not significant. This implies that the BRC has relative high resistance to temperature for a short time and the later does not affect the mechanical failure behavior.

Preprints (www.preprints.org) | NOT PEER-REVIEWED | Posted: 15 April 2019 doi:10.20944/preprints201904.0163.v1

Table 1: Young Modulus values of a butyl membrane exposed various temperatures

Exposure time (h)	Exposure temperature					
	80°C		100°C		120°C	
	E_{theo}	E_{exp}	E_{theo}	E_{exp}	E_{theo}	E_{exp}
0	4.08 (0.42)	3.40 (0.04)	3.78 (0.06)	3.00 (0.05)	4.80 (0.30)	4.11 (0.16)
1	3.90 (0.36)	2.89 (0.2)	3.93 (0.48)	3.15 (0.25)	6.57 (0.12)	6.10 (1.10)
2	3.99 (0.30)	3.01 (0.09)	3.90 (0.10)	3.20 (0.13)	8.12 0.24)	7.43 (0.18)
4	3.78 (0.24)	2.99 (0.03)	3.66 (0.36)	2.88 (0.18)	6.65 (0.66)	5.45 (0.85)
6	3.78 (0.42)	2.98 (0.10)	3.72 (0.04)	3.01 (0.02)	5.44 (0.18)	4.57 (0.02)
14	3.84 (0.24)	2.98 (0.09)	4.14 (0.09)	3.27 (0.01)	6.35 (0.36)	5.08 (0.14)
24	3.90 (0.36)	2.96 (0.02)	4.08 (0.09)	3.30 (0.09)	6.08 (0.16)	4.80 (0.12)

Note: between parentheses: standard deviation (SD)

3.2. Effect of simultaneous temperature and metalworking fluid on properties, structure and morphology

In the working condition, glove materials are often in contact with hot MWFs, generated by friction of machine devices. This factor could be directly affected on the protective performance of the glove materials. The effect of simultaneous temperature and MWFs on properties of butyl membranes is investigated. Figure 2a shows the variation of the constant C_1 as a function of expose temperature in the presence of a metalworking fluid (Milform 64 SST). As shown in Figure 2a, the changes of the constant C_1 with exposure time at 80°C are substantially similar to that at 100°C, thus these two curves are approximately superposed. However, at 120°C, the curve tendency is different when compared to that at lower exposure temperatures, where C_1 values dramatically drop at the first hours of exposure and then tends to archive a plateau region. Figure 2b shows the effect of temperature and MWFs on the constant C_2. It demonstrates that the constant C_2 is rapidly decreased with the exposure time and approach to zero after 24 hrs of exposition. Therefore, the cohesive strength of inter-chain eventually became weak [54] and the viscoelastic behavior may be also affected. The results are in good agreement with that observed by Gumbrell *et al.* [58] and Allen *et al.[59]* in studying the aging process of natural rubber to different solvents.

The calculation of the Young's modulus, in particular at 80 °C and 100 °C, highlights the effect of simultaneous temperature and contaminants on the rigidity of the material. A significantly decrease of Young's modulus as a function of exposure time was observed (Table 2). This could be attributed to the reduction of the cohesive strength of inter-chains. The rigidity of butyl at 120°C is unstable. The Young's modulus firstly increases, then decreases before achieving a plateau region.

Preprints (www.preprints.org) | NOT PEER-REVIEWED | Posted: 15 April 2019 doi:10.20944/preprints201904.0163.v1

This variation is possibly related to the changes in the cross-linking density (N) as shown in Figure 2c. This variation is due to the correlation between the constants C_1 and C_2. The similar behavior was also discussed by Nohilé et al.[4] demonstrating that the swelling of BRC by solvents led to an increase of the material rigidity due to the loss of fillers. The later leads to a reduction of the tensile strength of BRC as shown in Figures 2d. It can be seen from these figures that the mechanical properties of material are decreased whatever exposure temperatures are applied. The longer exposure time, the higher loss of mechanical is observed.

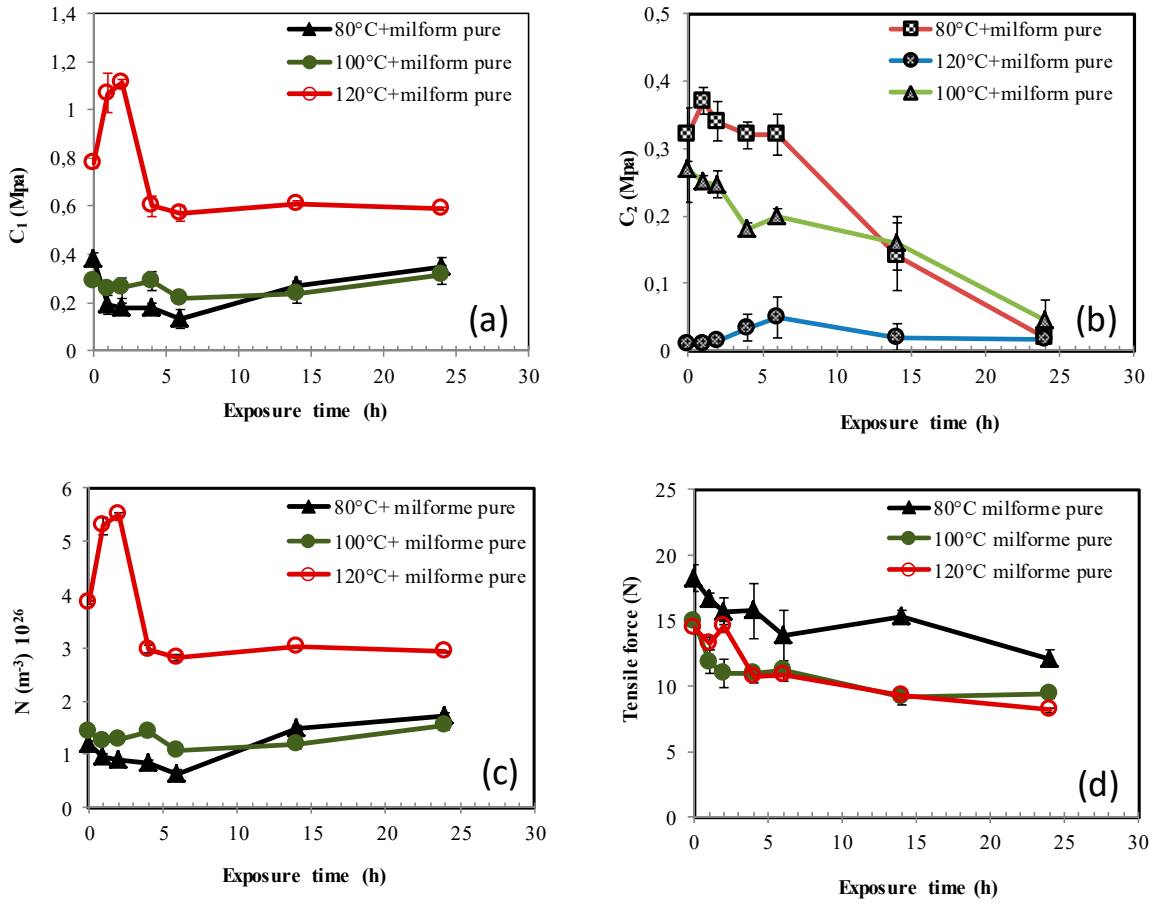

Figure 2 Effect of temperature and a MWF on mechanical properties of BRC as function of MWF exposure time a) constant C_1; b) constant C_2; c) crosslinking density (N); d) tensile force.

 doi:10.20944/preprints201904.0163.v1

Table 2: Young Modulus values of BRC membrane exposed at different temperatures in the presence of metalworking fluid

t (h)	Exposure temperatures					
	80°C		100°C		120°C	
	E_{theo}	E_{exp}	E_{theo}	E_{exp}	E_{theo}	E_{exp}
0	3.72	2.87	3.36	2.70	4.74	4.26
	(0.36)	(0.20)	(0.36)	(0.22)	(0.15)	(0.28)
1	3.36	2.64	3.03	2.51	6.76	6.28
	(0.36)	(0.16)	(0.12)	(0.09)	(0.54)	(0.17)
2	3.12	2.43	3.03	2.52	6.78	6.46
	(0.30)	(0.08)	(0.20)	(0.01)	(0.09)	(0.01)
4	3.00	2.41	2.82	2.33	3.804	3.26
	(0.24)	(0.05)	(0.30)	(0.11)	(0.36)	(0.18)
6	2.70	2.30	2.52	2.18	3.72	3.41
	(0.42)	(0.03)	(0.12)	(0.03)	(0.36)	(0.03)
14	2.46	2.31	2.40	2.01	3.66	3.15
	(0.24)	(0.05)	(0.48)	(0.05)	(0.18)	(0.04)
24	2.22	1.98	2.16	1.92	3.64	3.06
	(0.36)	(0.02)	(0.42)	(0.06)	(0.04)	(0.05)

Note: between parentheses: standard deviation (SD)

3.3. *Effect of temperature and MWF on dynamical Thermo-mechanical properties*

Dynamical thermo-mechanical analysis (DMTA) provides access to the elastic modulus and tangent values of materials. Figure 3a shows the example of Young modulus of BRC membrane before and after aging at 100 °C during 24 h in MWF (Milform 64SST). The curves are recorded from temperature -120 °C to 70°C. It shows that thermal degradation of membrane in metalworking fluid significantly reduces its Young modulus. It is clearly seen that the Young modulus is decreased from 1.45×10^7 to 4×10^6 MPa at -120 °C after aging at 100 °C for 24 h of exposure.

Preprints (www.preprints.org) | NOT PEER-REVIEWED | Posted: 15 April 2019 doi:10.20944/preprints201904.0163.v1

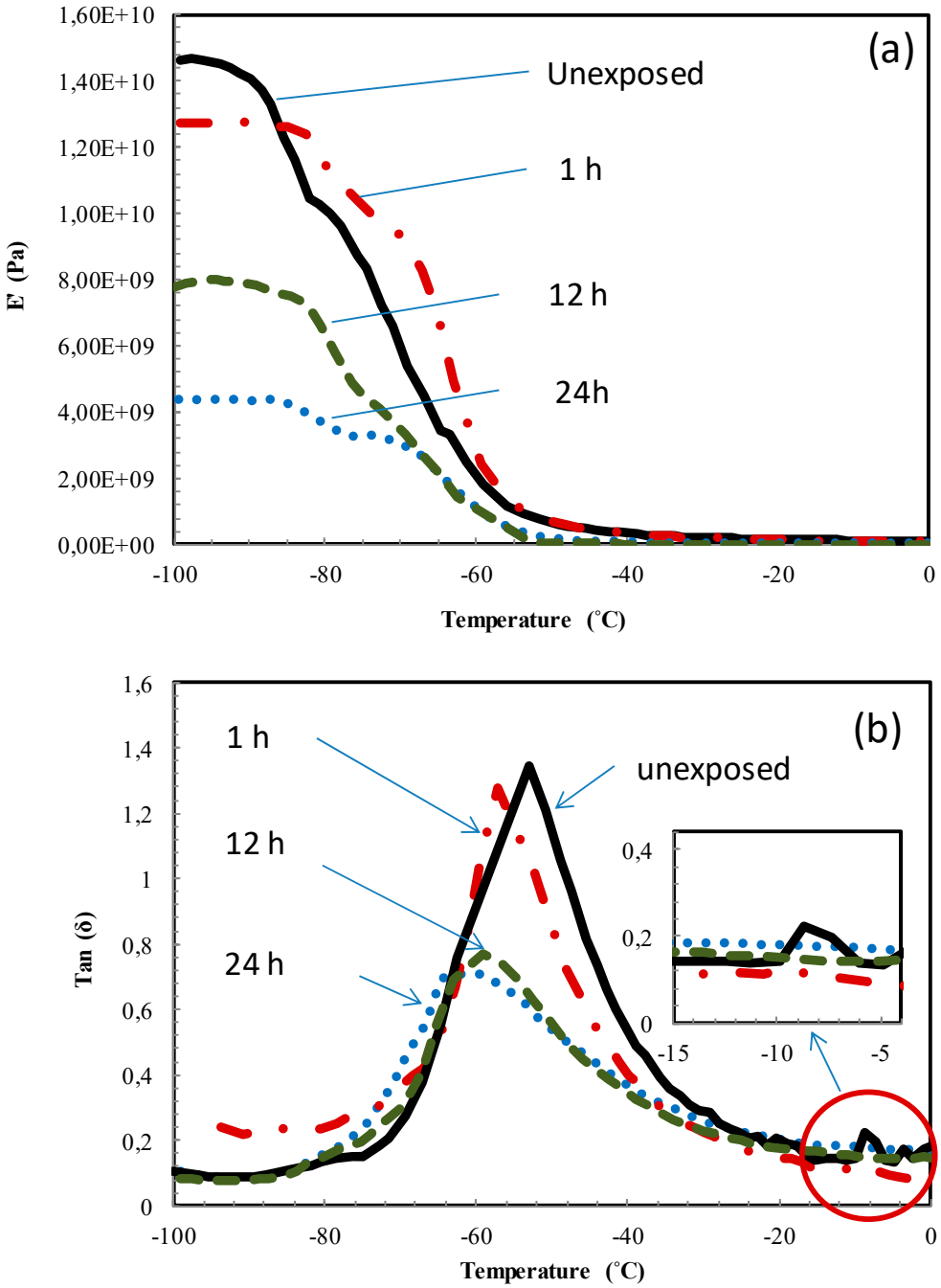

Figure 3 Evolution of storage modulus (a) and tangent delta values (b) of butyl rubber composite membrane before and after exposure in metalworking fluid (Milform 64 SST) at 100 °C during 24 h.

For an elastomer material, the glass transition temperature (T_g) is important factor that directly involves to the final properties of materials. This parameter is directly determined by DMTA curves, corresponding to the maximum peak of tan (δ). Figure 3b shows the example of the variation of tan (δ) of aged and un-aged samples at 100 °C with different aging times. It can be seen that the curve has a transition located around at - 45 °C, due to the glass transition temperature of butyl rubber. Another peak at a higher temperature at -8°C was also observed. This may be associated to movement of local molecular relaxations side [60, 61]. These local molecular movements not only affect the

 doi:10.20944/preprints201904.0163.v1

viscoelastic response, but also the mechanical properties (elastic modulus, plastic deformation) and also the diffusion of solvents in polymer matrix.

After aging at 100 °C in a metalworking fluid (Milform 64SST) for 24 h, a significant increase of the glass transition temperature value from - 45 ˚C to - 63 ˚C temperature was observed. This result is in good agreement with that in the literature in showing that there was a decrease of T_g of BRC during thermal aging in silicone oil [62]. The intensity of tan peak (δ) of aged sample is observed to be lower than that of the un-aged sample. The disappearance of the peak corresponding to the secondary transition temperature associated with the local molecular movement is observed in the aged sample. It can be attributed by the presence of MWF in elastomer matrix and leads to a better "molecular lubrication" due to the plasticization affect [63]. Regard to the reduction of T_g, since the glass transition temperature varies linearly with the molar mass and the molecular loss lead to a shift of the T_g to lower temperature areas [64]. The decrease of T_g observed this present study, is may be due to the thermal and chemical degradation of material by chains scissions that lead to a reduction of the molecular mass, that can explain the deterioration of mechanical properties of the material as shown in the previous section.

3.4. *Effect of temperature and MWF on morphology, thermal properties and service lifetime of butyl composites*

The scanning electron microscope was used to study the changes of the BRC membrane morphology during aging process. Figure 4 shows the SEM images of a sample of butyl before and after exposure in MWF. Figure 4 d shows that in the case of unexposed sample, a large distribution of fillers in the elastomer matrix is observed. However, these reinforcements are missing at the surface of exposed sample. The appearance of holes on the surface of the aged sample is also observed, this can be due to the removal of fillers that replaced by metalworking fluid (Fig. 4b). In other studies, the same damage was observed with bromobutyl rubber when they are undergone a thermal aging process [65]. The presence of MWF at elevated temperature, various micro cracks on the exposed sample (Fig. 4c) can be found due to the loss of reinforcements at the sample surface, generated by thermo-oxidation aging and plasticization effect. This observation is in good agreement the literature [65]. The appearance of micro-cracks on rubber materials is believed to derive from the nucleation effect of the dissolved vapor and gas in the low molecular weight domains of the rubber [66]. The loss of reinforcement is confirmed by thermogravimetric analysis (TGA) under argon atmosphere conditions. The thermal stability of BRC membrane was evaluated by thermo gravimetric analysis at the temperature range from 30 to 800˚C (Figure 5). The TGA curves show that the decomposition BRC evolves in the same way for both aged and un-aged samples. It found that the onset decomposition temperature of an original sample is about 205 °C with a residue of 52 % at 460 °C while the onset decomposition temperature for the aged one is about 228 ˚C with a residue of 42 % at 460 ˚C. In other words, the aged process leads to a reduction of carbon black filler from 52 % for original rubber to about 42 % for aged sample.

Preprints (www.preprints.org) | NOT PEER-REVIEWED | Posted: 15 April 2019 doi:10.20944/preprints201904.0163.v1

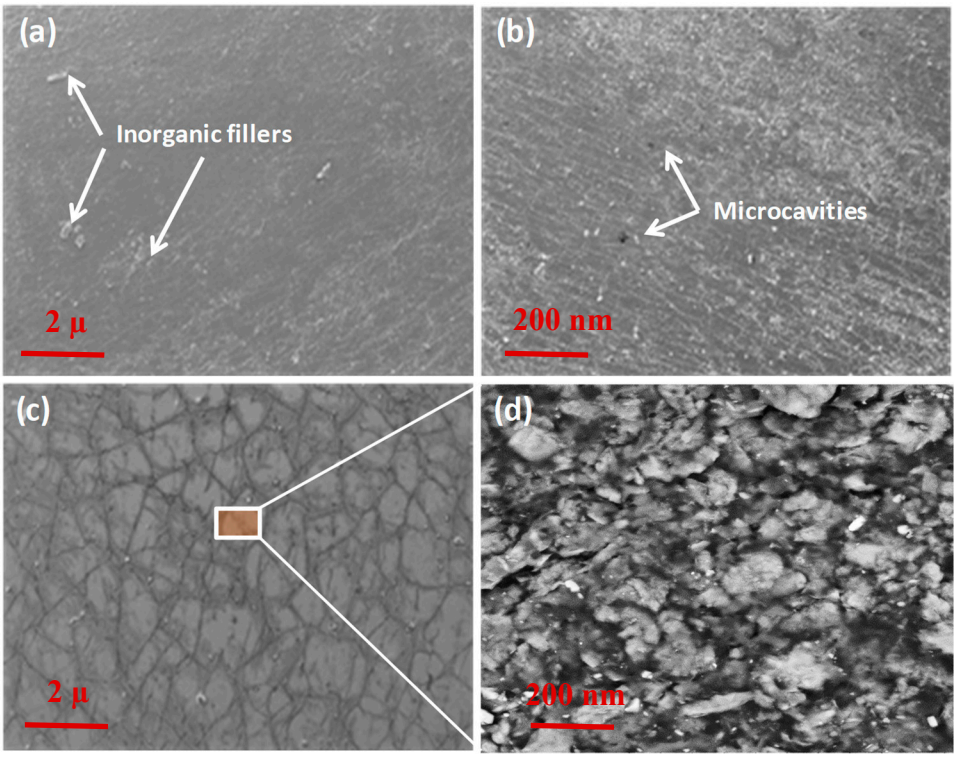

Figure 4 SEM images of butyl rubber composite membranes: a) non-aged sample, b) aged at 100 C, c) aged at 100 °C with the presence of a metalworking fluid (Milform 64 SST) during 24 hrs, c) higher magnification of image 4c, showing the rugosity of sample surface.

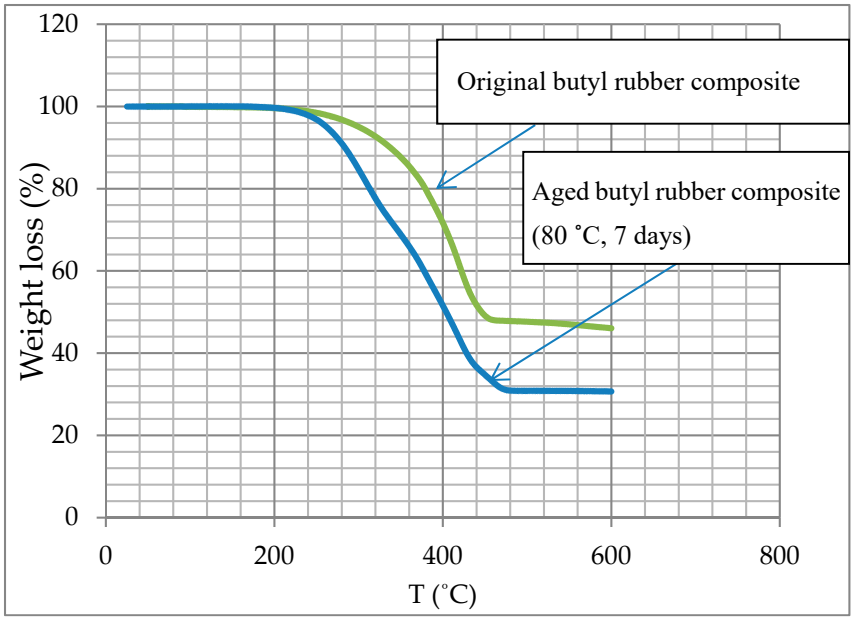

Figure 5 Thermogravimetric curves of butyl rubber composite before and after aged in Milform 64 SST at 80 °C during a week.

Preprints (www.preprints.org) | NOT PEER-REVIEWED | Posted: 15 April 2019 doi:10.20944/preprints201904.0163.v1

Changes in tensile force are observed at all studied temperatures (Figure 6). Indeed, after 24 hrs of exposure, the tensile force drops by about 23 % at 80 °C. Whereas it decreases by about 41 % at 120 °C. The results of tensile tests of BRC at different temperatures helps to give a prediction of the service life out by applying the Arrhenius model to the time-temperature data (Eq.9). In fact, the variation of rate of overall aging processes can be calculated from mentioned above equation (Eq.9). Where E is activation energy, R is universal constant (8.314 J/mol.K), T is absolute temperature and A is the pre-exponential factor. The curves describing the relationship between ln(t) vs 1/T should be linear and thus the activation energy and service life time can be calculated from this curve.

$$K = A \exp(-E/RT) \qquad \text{Eq.9}$$

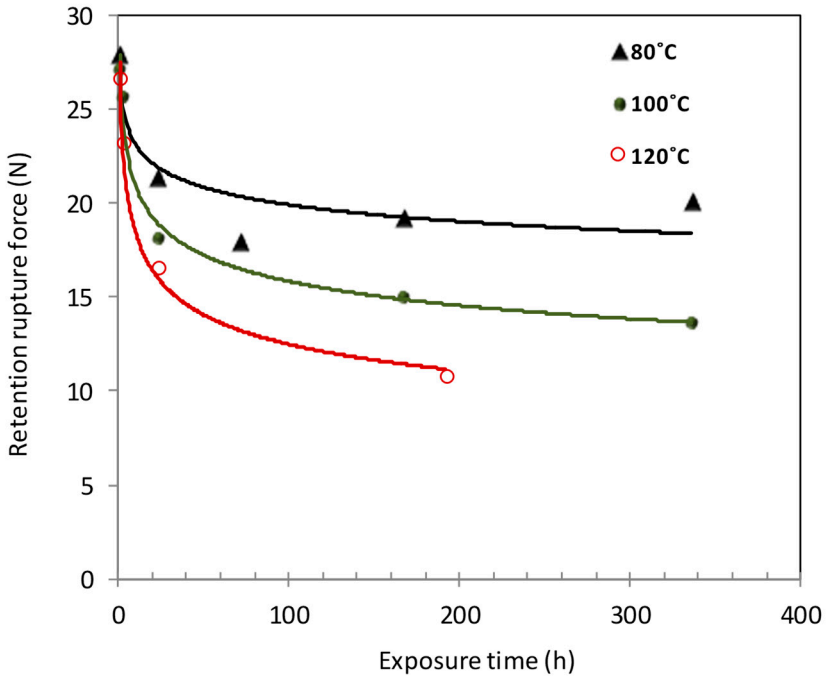

Figure 6 Variation of tensile force of BRC at different temperatures as a function of exposure time.

The definition of the end-used service lifetime of the material is still a subject in question in the literature. However, the assumption proposed by Rachid *et al.[67]* in which the material is considered run out when there is a reduction of about 50 % of tensile force seems to be acceptable. Here, were calculated the service life time for each aging temperature, using an empirical regression proposed method By El Aidani *et al*. [16, 67]. These lifetime values were exploited from Arrhenius curve, as shown in Figure 7, by plotting the logarithm of the lifetimes as a function of the inverse of the exposed temperatures. This Figure shows a good agreement with the *Arrhenius* model with high linear correlation coefficient ($R^2 = 0.95$). This indicates that the effect of thermal treatment between 80 and 120 °C on tensile force of BRC can be satisfactorily described by the Arrhenius model, which can therefore be used to predict the lifetime in this range of temperatures. The results of service life time of BRC can be found in Figure 6. An activation energy value of 157 $kJ.mol^{-1}$ was obtained from the

Preprints (www.preprints.org) | NOT PEER-REVIEWED | Posted: 15 April 2019 doi:10.20944/preprints201904.0163.v1

Arrhenius curve. That means, at 80 °C, the mechanical properties of BRC remains acceptable till 344 days while it drops to about 2 days at 120 °C.

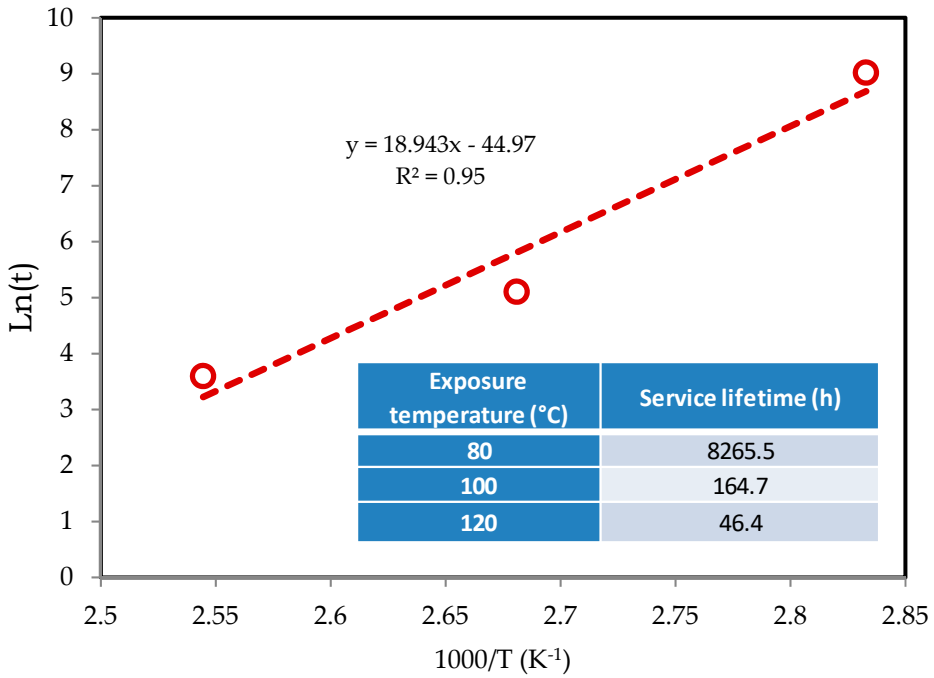

Exposure temperature (°C)	Service lifetime (h)
80	8265.5
100	164.7
120	46.4

Figure 7 Extrapolation of Arrhenius plot of BRC membrane based on tensile force. Insert: Predicted values of service lifetime, calculated from Arrhenius plot based on tensile force at different temperature.

4. Conclusions

The effect of temperature with and without MWFs on the evolution of mechanical and physico-chemical descriptors as well as structure of BRC is investigated. The Mooney-Rivlin's theory is used to determine the changes of physical and chemical bonds and the viscoelastic behavior of BRCs when they are in contact with a MWFs at high temperature via the determination of the elastic constant C_1 and C_2 at different temperatures ranging from 80 °C to 120 °C. The results show that temperature and MWFs lead to the decrease of elastic constant C_2, suggesting a decrease of the force of cohesion of polymer network. When BRC membranes are in contact with MWFs at high temperature, the irreversible behavior, related to intrinsic property of elastomers, is missing and significant changes in mechanical properties of material are observed.

The temperature is found to be accelerated the degradation process and the loss of mechanical properties of material was more pronounced at high temperature. The decrease of elasticity and reduction of the glass transition temperature of BRC is also observed, implying that BRC is not appropriated to use in oily working conditions, particularly in high temperature. In this case, gloves making from BRC must be changed more frequently to ensure an adequate protection level against mechanical and chemical risks. This work provides also useful information for rubber manufacturers to better understand the physicochemical degradation phenomena of their products under oily working conditions and thus improve the products quality.

Author Contributions: P.N.T has planned, supervised the works and written the manuscript. E.T has realized the experiments and participated to explain results. T.A.N. participated to edit the manuscript.

Funding: This research was funded by the *Institut de Recherche Robert-Sauvé en Santé et en Sécurité du Travail*, Quebec, Canada (Project R-983).

Acknowledgments: Thanks also to Prof. Jaime Lara (university of Montreal) for his constant support during this project.

Conflicts of Interest: The authors declare no conflict of interest.

5. References

1. Youssf, O., et al., *Cyclic Performance of Steel–Concrete–Steel Sandwich Beams with Rubcrete and LECA Concrete Core.* Journal of Composites Science, 2019. **3**(1): p. 5.
2. Youssf, O., et al., *Influence of Mixing Procedures, Rubber Treatment, and Fibre Additives on Rubcrete Performance.* Journal of Composites Science, 2019. **3**(2): p. 41.
3. Aguilar-Bolados, H., et al., *Removal of Surfactant from Nanocomposites Films Based on Thermally Reduced Graphene Oxide and Natural Rubber.* Journal of Composites Science, 2019. **3**(2): p. 31.
4. Nohilé, C., P.I. Dolez, and T. Vu-Khanh, *Mechanical and Chemical Effects of Solvent Swelling on Butyl Rubber.* 2010: p. 527-534.
5. Ebnesajjad, S., *8 - Characteristics of Adhesive Materials*, in *Handbook of Adhesives and Surface Preparation*, S. Ebnesajjad, Editor. 2011, William Andrew Publishing: Oxford. p. 137-183.
6. G. Pape, P., *15 - Adhesion Promoters*, in *Handbook of Adhesives and Surface Preparation*, S. Ebnesajjad, Editor. 2011, William Andrew Publishing: Oxford. p. 369-386.
7. Rabilloud, G., *12 - Adhesives for Electronics*, in *Handbook of Adhesives and Surface Preparation*, S. Ebnesajjad, Editor. 2011, William Andrew Publishing: Oxford. p. 259-299.
8. Rabilloud, G., *9 - Heat-Resistant Adhesives*, in *Handbook of Adhesives and Surface Preparation*, S. Ebnesajjad, Editor. 2011, William Andrew Publishing: Oxford. p. 185-220.
9. Fabris, H.J. and W.G. Knauss, *Synthetic Polymer Adhesives.* 1989: p. 131-177.
10. Haworth, J.P. and F.P. Baldwin, *Butyl Rubber Properties and Compounding.* Industrial & Engineering Chemistry, 1942. **34**(11): p. 1301-1308.
11. Ford, F.P. and A.M. Gessler, *Some Properties of Butyl Rubber-Carbon Black Systems.* Industrial & Engineering Chemistry, 1952. **44**(4): p. 819-824.
12. Yu, B.-C., et al., *A new approach for recycling waste rubber products in Li–S batteries.* Energy & Environmental Science, 2017. **10**(1): p. 86-90.
13. Xu, W. and S.S. Que Hee, *Permeation of a Metalworking Fluid Through a Latex Glove Under Field Use Conditions.* Bulletin of Environmental Contamination and Toxicology, 2009. **84**(1): p. 5.
14. Xu, W. and S.S. Que Hee, *Swelling of four glove materials challenged by six metalworking fluids.* Arch Environ Contam Toxicol, 2008. **54**(1): p. 1-8.
15. Nguyen-Tri, P., et al., *Swelling behavior of polymeric membranes to metalworking fluids.* Journal of Applied Polymer Science, 2018. **135**(3): p. 45717.
16. El Aidani, R., et al., *Photochemical aging of an e-PTFE/NOMEX® membrane used in firefighter protective clothing.* Polymer Degradation and Stability, 2013. **98**(7): p. 1300-1310.
17. Nguyen-Tri, P., et al., *Chemical ageingaging of a polyester nonwoven membrane used in aerosol and drainage filter.* Polymer Degradation and Stability, 2014. **101**: p. 71-80.
18. Nguyen, T.V., et al., *Accelerated degradation of water borne acrylic nanocomposites used in outdoor protective coatings.* Polymer Degradation and Stability, 2016. **128**: p. 65-76.

19. Nguyen, T.P., *Nanoscale analysis of the photodegradation of Polyester fibers by AFM-IR* Journal of Photochemistry and Photobiology A: Chemistry, 2018. **Accepted**.
20. Nguyen, T.V., et al., *Stability of acrylic polyurethane coatings under accelerated aging tests and natural outdoor exposure: The critical role of the used photo-stabilizers.* Progress in Organic Coatings, 2018. **124**: p. 137-146.
21. Nguyen-Tri, P., et al., *Nanocomposite Coatings: Preparation, Characterization, Properties, and Applications.* International Journal of Corrosion, 2018. **2018**: p. 1-19.
22. Nguyen-Tri, P. and R.E. Prud'homme, *Nanoscale analysis of the photodegradation of polyester fibers by AFM-IR.* Journal of Photochemistry and Photobiology A: Chemistry, 2019. **371**: p. 196-204.
23. Nguyen-Tri, P., et al., *Recent progress in the preparation, properties and applications of superhydrophobic nano-based coatings and surfaces: A review.* Progress in Organic Coatings, 2019. **132**: p. 235-256.
24. Ouellet-Plamondon, P.N.T.S.R.C., *Nanomaterials-Based Coatings : Fundamentals and Applications*. Vol. 1. 2019: Elsevier. 474.
25. Tri Phuong, N., V. Gilbert, and B. Chuong, *Preparation of Recycled Polypropylene/ Organophilic Modified Layered Silicates Nanocomposites Part I: The Recycling Process of Polypropylene and the Mechanical Properties of Recycled Polypropylene/Organoclay Nanocomposites.* Journal of Reinforced Plastics and Composites, 2008. **27**(18): p. 1983-2000.
26. Nguyen Tri, P. and V. Gilbert, *Non-isothermal Crystallization Kinetics of Short Bamboo Fiber-reinforced Recycled Polypropylene Composites.* Journal of Reinforced Plastics and Composites, 2010. **29**(17): p. 2576-2591.
27. Nguyen Tri, P., C. Sollogoub, and A. Guinault, *Relationship between fiber chemical treatment and properties of recycled pp/bamboo fiber composites.* Journal of Reinforced Plastics and Composites, 2010. **29**(21): p. 3244-3256.
28. Boukehili, H. and P. Nguyen-Tri, *Helium gas barrier and water absorption behavior of bamboo fiber reinforced recycled polypropylene.* Journal of Reinforced Plastics and Composites, 2012. **31**(23): p. 1638-1651.
29. Nguyen Tri, P., A. Guinault, and C. Sollogoub, *Élaboration et propriétés des composites polypropylène recyclé/fibres de bambou.* Matériaux & Techniques, 2012. **100**(5): p. 413-423.
30. Triki, E., et al., *Investigation of tearing mechanisms of woven textile.* Polymer Composites, 2012. **33**(9): p. 1578-1585.
31. Triki, E., et al., *Mechanics and mechanisms of tear resistance of woven fabrics.* Theoretical and Applied Fracture Mechanics, 2012. **61**: p. 33-39.
32. Tri, P.N., et al., *Crystallization behavior of poly(lactide)/poly(β-hydroxybutyrate)/talc composites.* Journal of Applied Polymer Science, 2013. **129**(6): p. 3355-3365.
33. Triki, E., et al., *Combined puncture/cutting of elastomer membranes by pointed blades: Characterization of mechanisms.* Journal of Applied Polymer Science, 2015. **132**(26): p. n/a-n/a.
34. Azizi, S., et al., *Electrical and thermal phenomena in low-density polyethylene/carbon black composites near the percolation threshold.* Journal of Applied Polymer Science, 2018: p. 47043.
35. Azizi, S., et al., *Electrical and thermal conductivity of ethylene vinyl acetate composite with graphene and carbon black filler.* Polymer Testing, 2018. **72**: p. 24-31.
36. Nguyen Tri, P. and R.E. Prud'homme, *Crystallization and Segregation Behavior at the Submicrometer Scale of PCL/PEG Blends.* Macromolecules, 2018. **51**(18): p. 7266-7273.

37. Satyabrata, M.T., Anh Nguyen; Phuong, Nguyen-Tri;, *Noble Metal-Metal Oxide Hybrid Nanoparticles*. Vol. 1. 2018: Elsevier.
38. Duc Chinh, V., et al., *Synthesis of Gold Nanoparticles Decorated with Multiwalled Carbon Nanotubes (Au-MWCNTs) via Cysteaminium Chloride Functionalization.* Scientific Reports, 2019. **9**(1): p. 5667.
39. Nguyen Tri, P., et al., *Antibacterial Behavior of Hybrid Nanoparticles.* 2019: p. 141-155.
40. Nguyen Tri, P., et al., *Methods for Synthesis of Hybrid Nanoparticles.* 2019: p. 51-63.
41. Nguyen-Tri, P., V. Nguyen, and T. Nguyen, *Biological Activity and Nanostructuration of Fe3O4-Ag/High Density Polyethylene Nanocomposites.* Journal of Composites Science, 2019. **3**(2): p. 34.
42. Ben Hassine, M., et al., *Time to failure prediction in rubber components subjected to thermal ageing: A combined approach based upon the intrinsic defect concept and the fracture mechanics.* Mechanics of Materials, 2014. **79**: p. 15-24.
43. Syed, I.H., et al., *Nonlinearity in the Mechanical Response of Rubber as Investigated by High-Frequency DMA.* Polymers (Basel), 2019. **11**(4).
44. Xiang, K., et al., *Investigation on the thermal oxidative aging mechanism and lifetime prediction of butyl rubber.* Macromolecular Research, 2013. **21**(1): p. 10-16.
45. Haghtalab, A. and S. Rahimi, *Study of viscoelastic properties of nanocomposites of SiO2-acrylonitrile-butadiene-styrene.* Journal of Applied Polymer Science, 2013. **127**(6): p. 4318-4327.
46. Lewicki, J.P., et al., *Degradative Thermal Analysis and Dielectric Spectroscopy Studies of Aging in Polysiloxane Nanocomposites.* 2009. **1004**: p. 239-254.
47. Rivlin, R.S., *Large Elastic Deformations of Isotropic Materials. IV. Further Developments of the General Theory.* Philosophical Transactions of the Royal Society A: Mathematical, Physical and Engineering Sciences, 1948. **241**(835): p. 379-397.
48. Rivlin, R.S., *Large Elastic Deformations of Isotropic Materials. I. Fundamental Concepts.* Philosophical Transactions of the Royal Society A: Mathematical, Physical and Engineering Sciences, 1948. **240**(822): p. 459-490.
49. Arimoto, H., *α–γ Transition of nylon 6.* Journal of Polymer Science Part A: General Papers, 1964. **2**(5): p. 2283-2295.
50. Slichter, W.P., *Molecular motion in polyamides.* Journal of Polymer Science, 1959. **35**(128): p. 77-92.
51. Hagen, R., L. Salmén, and B. Stenberg, *Effects of the type of crosslink on viscoelastic properties of natural rubber.* Journal of Polymer Science Part B: Polymer Physics, 1996. **34**(12): p. 1997-2006.
52. Gordon, M., *The Physics of Rubber Elasticity (Third Edition). L. R. G. Treloar, Clarendon Press, Oxford. 1975 pp. xii + 370. Price: £14.00.* British Polymer Journal, 1976. **8**(1): p. 39-39.
53. Sombatsompop, N., *Investigation of Swelling Behavior of NR Vulcanisates.* Polymer-Plastics Technology and Engineering, 1998. **37**(1): p. 19-39.
54. Mark, J.E., *Experimental Determinations of Crosslink Densities.* Rubber Chemistry and Technology, 1982. **55**(3): p. 762-768.
55. Priss, L.S., *Molecular origin of constants in the theory of rubber-like elasticity considering network chains steric interaction.* Pure and Applied Chemistry, 1981. **53**(8): p. 1581-1596.
56. Mark, J.E., *The Constants 2C1and 2C2in Phenomeno-Logical Elasticity Theory and Their Dependence on Experimental Variables.* Rubber Chemistry and Technology, 1975. **48**(3): p. 495-512.
57. Ha-Anh, T. and T. Vu-Khanh, *Prediction of mechanical properties of polychloroprene during thermo-oxidative aging.* Polymer Testing, 2005. **24**(6): p. 775-780.

58. Gumbrell, S.M., L. Mullins, and R.S. Rivlin, *Departures of the elastic behaviour of rubbers in simple extension from the kinetic theory.* Transactions of the Faraday Society, 1953. **49**(0): p. 1495-1505.
59. Allen, G., et al., *Thermodynamics of rubber elasticity at constant volume.* Transactions of the Faraday Society, 1971. **67**(0): p. 1278-1292.
60. Dutta, N.K., D. Khastgir, and D.K. Tripathy, *The effect of carbon black concentration on the dynamic mechanical properties of bromobutyl rubber.* Journal of Materials Science, 1991. **26**(1): p. 177-188.
61. García, M., I. Garmendia, and J. García, *Influence of natural fiber type in eco-composites.* Journal of Applied Polymer Science, 2008. **107**(5): p. 2994-3004.
62. Ali, S., et al., *Thermal and Thermo-Mechanical Behavior of Butyl based Rubber Exposed to Silicon Oil at Elevated Temperature.* Journal of the Chemical Society of Pakistan, 2013. **35**(6): p. 1437-1444.
63. Barrere, C. and F. Dal Maso, *Résines époxy réticulées par des polyamines : structure et propriétés.* Revue de l'Institut Français du Pétrole, 2006. **52**(3): p. 317-335.
64. Fox, T.G. and P.J. Flory, *Second-Order Transition Temperatures and Related Properties of Polystyrene. I. Influence of Molecular Weight.* Journal of Applied Physics, 1950. **21**(6): p. 581-591.
65. G K Kannan, L.V.G., L Nirmala and N S Kumar, *Thermal ageing studies of bromo-butyl rubber used in NBCpersonal protective equipment.* Journal of Scientific & Industrial Research, 2010. **69**: p. 841-849.
66. Grandcoin, J., A. Boukamel, and S. Lejeunes, *A micro-mechanically based continuum damage model for fatigue life prediction of filled rubbers.* International Journal of Solids and Structures, 2014. **51**(6): p. 1274-1286.
67. El Aidani, R., P.I. Dolez, and T. Vu-Khanh, *Effect of thermal aging on the mechanical and barrier properties of an e-PTFE/Nomex® moisture membrane used in firefighters' protective suits.* Journal of Applied Polymer Science, 2011. **121**(5): p. 3101-3110.